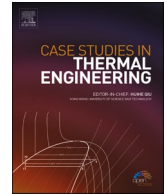




ELSEVIER

Contents lists available at ScienceDirect

## Case Studies in Thermal Engineering

journal homepage: [www.elsevier.com/locate/csife](http://www.elsevier.com/locate/csife)

# Thermal performance investigation of double pipe heat exchanger embedded with extended surfaces using nanofluid technique as enhancement

Mohammed Flyyih Hasan<sup>a</sup>, Merdin Danişmaz<sup>a</sup>, Bassim Mohammed Majel<sup>b,\*</sup>

<sup>a</sup> Kirsehir Ahi Evran University, Sciences Mechanical Engineering Department, 32200, Turkey

<sup>b</sup> Department of Refrigeration and Air Conditioning Engineering, Al-Rafidain University College, Baghdad, 10001, Iraq

## ARTICLE INFO

Handling Editor: Huihe Qiu

### Keywords:

Double pipe heat exchanger  
Extended surface  
Nanofluid

## ABSTRACT

In the present work, a numerical investigation of heat transfer enhancement in a “double pipe heat exchanger” embedded with an extended surface on the inner tube’s outer surface with the addition of “Alumina nanofluid” has been carried out. Through the annuli, water with varying mass flow rates (0.03–0.07 kg/s) and hot de-ionized water with varying Reynolds numbers (250–2500) flows, while hot de-ionized water flows through the inner tube. One type of nanoparticle ( $Al_2O_3$ ) having volume concentrations (1%, 3%, and 5%) was used during simulation. Numerical analysis was performed using Computational Fluid dynamics, and the Solid works was used to generate the model. A Semi-Implicit Method for Pressure Linked Equations technique was used to solve the governing equations and discretized using the finite volume method. The simulated results show that the use of a finned tube heat exchanger resulted in an improvement ratio between (2.3) and (3.1). The coefficient of convective heat transfer increased numerically as the volume concentration and Reynolds number increased. The heat transfer coefficient and thermal conductivity rise by 20% and 4.7%, respectively, at a volume concentration of 5%.

## 1. Introduction

Thermal systems are now among the most vital technical systems. Several techniques have been investigated and developed in order to improve heat transfer in these systems and achieve a high level of thermal performance. Utilizing a number of surface-enhancement-based approaches, the heat transfer rate of traditional heat exchangers may be enhanced. This enhancement in heat transfer rate results from the circumstances provided by the use of improved surfaces. These circumstances inhibit the establishment of the boundary layer, increase the turbulence level, expand the heat transfer area, and produce swirling and/or secondary flows. Enhanced heat transfer surfaces have several purposes for their use. Enhanced surfaces help reduce the size of heat exchangers, which could lead to a reduction in their costs. In addition, they decrease the pumping power that is required for certain thermal exchange processes. Moreover, they increase the heat transfer coefficient value (UA) of heat exchangers, which assists in either obtaining “an increased heat exchange rate for fixed fluid inlet temperatures or reducing the mean temperature difference for the heat exchange. In turn, this improves the effectiveness and efficiency of thermal processes and results in operating cost savings [1]. The heat exchanger industry has been striving for improved thermal contact (enhanced heat transfer coefficient) and reduced pumping power in order to improve the thermohydraulic efficiency of heat exchangers [2]. The use of a finned tube to increase heat transmission is becoming

\* Corresponding author.

E-mail address: [basim.mohammed@ruc.edu.iq](mailto:basim.mohammed@ruc.edu.iq) (B.M. Majel).

<https://doi.org/10.1016/j.csife.2023.102774>

Received 23 November 2022; Received in revised form 17 January 2023; Accepted 23 January 2023

Available online 4 February 2023

2214-157X/© 2023 The Authors. Published by Elsevier Ltd. This is an open access article under the CC BY-NC-ND license (<http://creativecommons.org/licenses/by-nc-nd/4.0/>).

more important in a growing number of industrial applications; thus, the finned tube has been the subject of several studies. **Sivakumar and Rajan** [3] studied the heat transfer and efficiency of a double-pipe heat exchanger with two flow directions: parallel flow and counter flow. Consider the flow in these two directions to be laminar and use the exit temperatures of both hot and cold fluid with various mass flow rates from the experimental setup. Work out the parallel flow heat exchanger's heat transfer and efficiency, then compare these results to those for the counter flow heat exchanger. For this study, Ansys Fluent Version, a commercial CFD package, was used. Generate and mesh the 3D model of the heat exchanger. Last but not least, the numerical values validate the experimental assessment. **Sahiti et al.** [4] experimentally investigate the increase of heat transmission using pin fins. Utilizing tiny cylindrical pins on the surface of the heat exchanger revealed a significant improvement. Simple relationships between convection and conduction heat transfer were utilized to create an equation revealing the factors influencing heat transfer enhancement. It was able to increase the Nusselt number in their investigation by utilizing a pin element as opposed to a smooth tube heat exchanger. **Shuai and Chang** [5] Performing a three-dimensional numerical simulation on an integrated pin–fin tube heat exchanger utilizing fluid software. They confirmed that the program for numerical simulation of integral pin–fin tubes is possible. It has been shown that Fluent software can do numerical simulations on integral pin–fin tubes and is a useful tool for designing and developing heat exchange tubes. **Dong et al.** [6] conducted research to determine how perforated circular finned tubes affect convective heat transfer in circular finned tube heat exchangers. For the 2 holes and 4 holes examples, respectively, the convective heat transfer coefficient rose by 3.55 and 3.31%, while the pressure drop increased by 0.68 and 2.08%. **Nagarani and Mayilsamy** [7] conducted an experimental investigation and study of the heat transfer rate and efficiency for circular and elliptical annular fins in various climate conditions. It was concluded that the elliptical fin was superior to the circular fin. Space, time, flow conditions, and fluid parameters influence the heat transfer coefficient. Changes in environmental conditions affect the efficiency and coefficient of heat transfer. **Senthilraja and Vijayakumar** [8] Utilizing a twin pipe heat exchanger, the heat transfer coefficient of CuO/Water nanofluid was experimentally determined. To make a nanofluid, CuO particles were distributed in deionized water. At varied volume concentrations, the nanofluid has a diameter of 27 nm at room temperature (0.1% and 0.3%). It was discovered that as time passes, the heat transfer coefficient rises, whereas an increase in the liquid flow rate causes the Nusselt number to rise. The nanofluid with a concentration of 0.3% had the greatest heat transfer coefficient. **Heris et al.** [9] conducted a prepared experimental examination of laminar convective heat transmission of CuO and Cu nanoparticles with respective diameters of 20, 50–60, and 25 nm. Through a circular tube with a fixed wall temperature, water was employed as the base fluid. The heat transfer coefficient was calculated for (0.2–3.0) percent volume concentrations of "(Cu, Al<sub>2</sub>O<sub>3</sub>, and CuO)" nanoparticles at various numbers of Peclet. The experimental data showed a good increase in the rate of heat transfer. This enhancement was related to the increase in the Peclet number and volume concentration for each nanofluid. The results were greater than the theoretical correlations predicted. The existence of an optimal concentration for each nanofluid regarding the best enhancement was obtained. **Lai et al.** [10] conducted an experimental investigation of alumina nanofluid flowing inside a (1 mm) diameter pipe made from stainless steel under constant heat flux conditions ( $Re < 270$ ). For a 11 percent volume concentration, the Nusselt number increased by 8%. **Farajollahi et al.** [11] conducted an experimental investigation of "Al<sub>2</sub>O<sub>3</sub>/water and TiO<sub>2</sub>/water nanofluids" in a heat exchanger type shell-and-tube operating under conditions of turbulent flow. The influence of the number of Peclet, volume concentration of particles, and type of particle on the heat transmission properties was studied. According to the findings, the addition of nanoparticles to the basefluid significantly improved heat transmission. Various volume fractions were used. Comparing the behavior of two nanofluids revealed that the optimal concentration of TiO<sub>2</sub>/water nanofluid had superior heat transfer properties. In addition, the heat transmission properties of Al<sub>2</sub>O<sub>3</sub>/water nanofluid improve as the concentration of nanoparticles increases. **Esmailzadeh et al.** [12] examined the hydrodynamics and heat transfer properties of 15 nm-sized Al<sub>2</sub>O<sub>3</sub>- nanoparticles in laminar flow with continuous heat flux within a circular tube. The impact of varying volume concentrations on the enhancement of heat transfer and friction factor was tested, proving that as the particle volume fraction increased, the heat transfer coefficient increased as well. The average heat transfer coefficient increased in comparison to distilled water by 6.8% at a volume concentration of 0.5% and by 19.1% at a volume concentration of 1%, according to the results. Also, the change in friction factor was negligible. **Mathanraj et al.** [13] conducted an experiment to compare and examine the heat transfer for counterflow of twin pipe heat exchangers with and without longitudinal triangular fins. The test section includes a horizontal copper tube of 1000 mm in length with an inner diameter of 15 mm and an outside diameter of 19 mm. The triangular fin has dimensions of 8 mm in height, 9 mm in width, and 2 mm in depth. Examining the effects of mass flow rates and fin spacing on a heat exchanger's thermal efficiency. The obtained results indicate that raising the mass flow rate of cold fluids increases the efficiency and heat transfer rate. Throughout the experiment, the total heat transfer coefficient and the logarithmic mean temperature difference both grow. **Córcoles et al.** [14] carried out numerical analysis to study the effect of geometrical factors on a heat exchanger with two pipes that have eight inner corrugated tubes. Turbulent flow condition has been considered ( $Re = 25,000$ ), and the Realizable  $k-\epsilon$  turbulence model of a 3-D unstructured tetrahedral mesh scheme was analyzed and validated with an experimental results. The simulated data show that the case study of lowest helical pitch ( $P/D = 0.682$ ) and highest corrugation height ( $H/D = 0.05$ ) presented the largest pressure drops in both the annular and inner tubes. The maximum number of transfer units reaches to 29% compared with the flat tube. **Mahmud and Rawand** [15] conducted an experimental study to address the effect of the twisting for inner pipe on a double-pipe heat exchanger's thermal efficiency. Various twisting numbers (3, 5, and 7 twists per unit length) in both counter and parallel flow directions are examined. All cases are conducted under a turbulent flow regime ( $Re = 5000-26000$ ) using water as a working fluid. The experimental data show that there is an enhancement in the thermal performance for all three twisting pipes. The highest Nusselt number augmentation factor is found to be 2.2 for the counter flow and 1.8 for the parallel flow as compared to the flat pipe. The maximum enhancement factor are observed at ( $Re = 26,000$ ) for both flow directions. Clearly, the literature is vast, but there is a dearth of information about the use of nanofluids to improve the performance of finned tube heat exchangers. **Mojtaba et al.** [16] studied the fluid flow in a shell and tube heat exchanger using Carreau- Yasuda non-Newtonian fluid. The heat equation for thick tubes, the heat equation for RT-35 as a non-Newtonian Carreau-Yasuda fluid, the

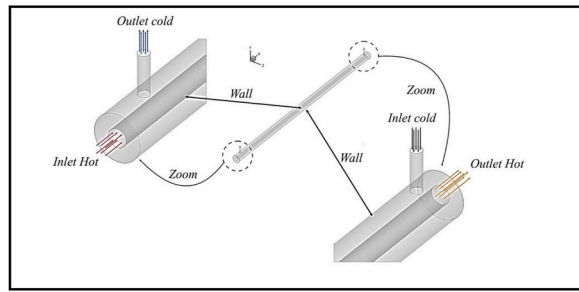


Fig. 1. The model geometry used in the simulations of plain tube.

horizontal and vertical directions, and the continuity and momentum equations were determined and transformed into their non-dimensional forms, and then solved using the finite element method. The findings showed that higher porosity parameter values resulted in slower heat transfer rates, which in turn weakened the PCM melting front. Additionally, it was discovered that altering the center-to-center separation between the hot tubes had an impact on how the melting front propagated. Through CFD, Do et al. [17] looked into the characteristics of turbulent heat transfer in double pipe heat exchangers. Following that, the impact of inner pipe geometry on flow and heat transfer was examined. The effects of inner pipe geometry on thermal characteristics were primarily discovered to be strongly influenced by the value of  $Re_{\text{pipe}}$ . Using flat inner pipes with a low aspect ratio improves overall heat transfer, thermal efficiency, and performance index for  $Re_{\text{pipe}} < 7000$ . These findings suggest that flat inner pipes with small aspect ratios are preferred for double-pipe heat exchanger performance enhancement at low Reynolds numbers, while circular inner pipes remain the best option at high Reynolds numbers.

This study used computational fluid dynamics (CFD) simulation to examine how the inner pipe's embedded (U) fin shape affects the efficiency of double-pipe heat exchangers. When compared to the predicted correlations in the literature, CFD can more precisely and affordably explain the intricate flow and heat transfer patterns inside double-pipe heat exchangers. To predict flow fields and heat transfer with and without nanofluids using a single type of oxide nanoparticle ( $Al_2O_3$ ), the current heat exchanger will be numerically simulated using the ANSYS Fluent 20 software. This investigation is conducted at Reynolds numbers ranging from 250 to 2500 with an inner diameter of 20.4 mm. Several volume concentrations (1%, 3%, and 5%) have been applied to alumina nanoparticles. Finally, the influence of the inner pipe's U fins' geometry on pressure drop, temperature distribution, and thermal performance is investigated.

## 2. Numerical simulation

The ability of engineers to solve extremely complex engineering problems has improved due to the rapid development of numerical techniques and software, such as CFD codes. CFD codes are a useful tool for more accurate heat and fluid flow modeling used for understanding the complex hydrodynamics in many industrial processes. Many attempts have been made to analyze the intricate flows and heat exchange processes that occur inside the tube and to create heat transfer improvement devices using CFD modeling. In the current study, CFD modeling using the "FLUENT 20 package" was used to perform numerical simulation over a three-dimensional model of a heat exchanger. Utilizing the solutions of continuity, momentum, and energy conservation equations, the flow field within the heat exchanger is analyzed. The heat transmission of a smooth, finned tube with and without nanofluids is compared.

The second-order upwind scheme was used for the discretization of convection terms, energy, and turbulent kinetic and turbulent dissipation energy. The tri, tetra, and polyhedral mesh flow domains are particularly well-suited for this method's accuracy, stability, and convergence [18]. ANSYS-Fluent provides the option to choose among five pressure-velocity coupling algorithms: SIMPLE, SIMPLEC, PISO, Coupled, and [for unsteady flows using the non-iterative time advancement scheme (NITA)] Fractional Step (FSM). All the aforementioned schemes, except the "coupled" scheme, are based on the predictor-corrector. The SIMPLE algorithm was applied to the current cases to resolve the coupling between the velocity and pressure fields. The technique for computing pressure known as SIMPLE-the Semi-Implicit Method for Pressure-Linked Equations-is precise and gaussian. The velocity field for  $u$ ,  $v$ , and  $w$  is generally calculated along with the discretization of the momentum equation for the entire domain under the assumption of a known pressure distribution. If the velocity distribution satisfies the continuity equation, the solution is then demonstrated; if not, a new pressure distribution should be suggested, and so on. To accomplish this, the momentum equation and the proper corrections for the pressure field can be used [19]. In the subsequent parts, numerical approach will be elucidated.

### 2.1. Geometry

This work's geometries comprise a twin pipe heat exchanger and expanded surfaces with inlet and outlet parts for tubes holding hot and cold water and are drawn using "SOLID WORK PREMIUM 2020." The Annulus outer pipe is insulated.

### 2.2. Computational domain

In the current work, computational domains are shown as the inlet and exit of the hot water side in the inner tube and the cold water side in the annuli. Fins are constructed on the outer surface of the inner tube, and the flow on both sides is counter and then parallel, as seen in Fig. 1.

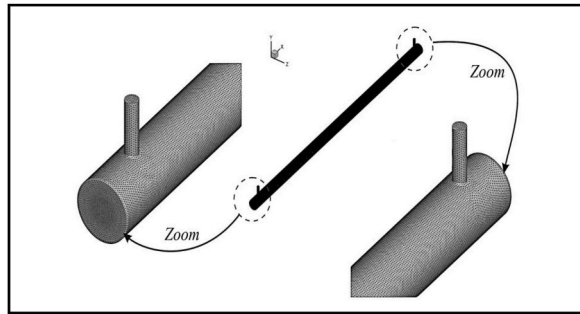


Fig. 2. Mesh of present model with plain tube.

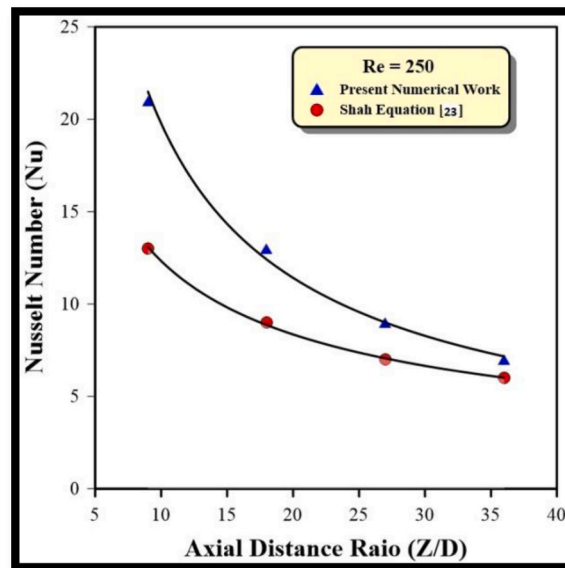


Fig. 3. Comparison between numerical work and Shah equation.

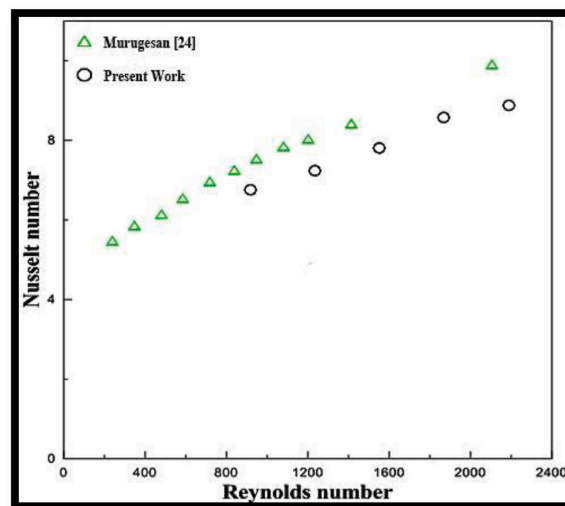


Fig. 4. Comparison of numerical (Nu) of study and the experimental work.

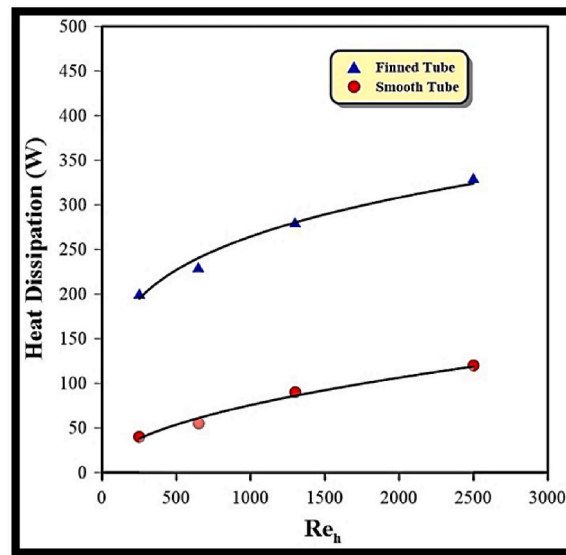


Fig. 5. Influence of the Reynolds number of hot water on heat dissipation at  $\dot{m}_c = 0.025$  kg/s.

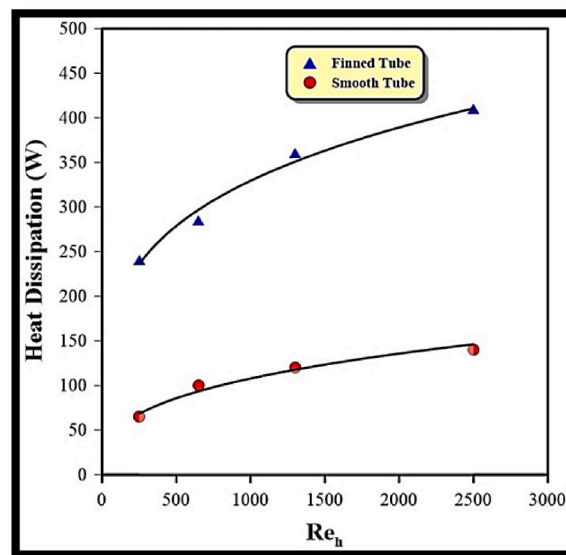


Fig. 6. Influence of the Reynolds number of hot water on heat dissipation at  $\dot{m}_c = 0.045$  kg/s.

### 2.3. Mesh generation

Using the finite-volume approach, the computational domain is discretized into a restricted number of control volumes using an unstructured mesh in the present study. Structured mesh is ruled out since it is beneficial for basic cases but insufficient and time-consuming for complicated geometries [20]. The model was meshified using the GAMBIT program. The refinement and development of mesh systems are crucial for predicting heat transport in complex geometries. Consequently, the density and dispersion of the mesh lines play significant roles in determining the precision. See Fig. 2.

### 3. Governing equations

Lars Davidson [21] and M. Izadi [22] describe the “governing equations for continuity,” “momentum,” and “energy of laminar flow” in a tube and turbulent flow in annuli.

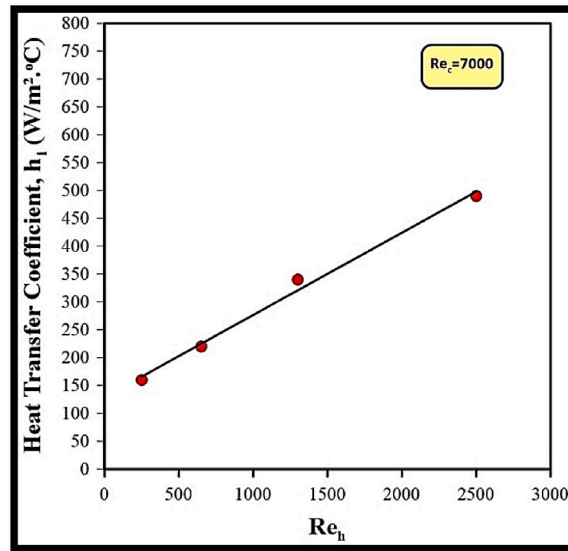


Fig. 7. ( $Re_h$ ) influence on the coefficient of heat transfer for a tube with fins at  $Re_c = 7000$ .

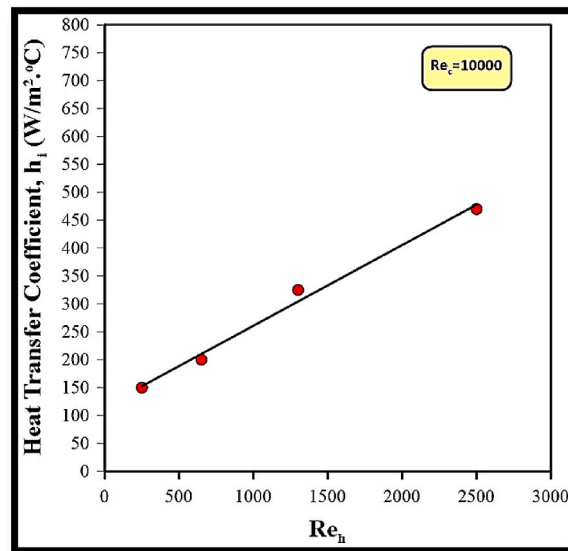


Fig. 8. ( $Re_h$ ) influence on the coefficient of heat transfer for a tube with fins at  $Re_c = 10,000$ .

### 3.1. 1 Laminar flow

The following governing equations must be solved for laminar flow in an inner tube.

#### 1. Conservation of Mass Equation

$$\frac{\partial u}{\partial x} + \frac{\partial v}{\partial x} + \frac{\partial w}{\partial x} = 0 \tag{3-1}$$

#### 2. Navier-Stokes equations Equation

$$\rho \left( u \frac{\partial u}{\partial x} + v \frac{\partial u}{\partial y} + w \frac{\partial u}{\partial z} \right) = - \frac{dp}{dx} + \mu \left( \frac{\partial^2 u}{\partial x^2} + \frac{\partial^2 u}{\partial y^2} + \frac{\partial^2 u}{\partial z^2} \right) \tag{3-2}$$

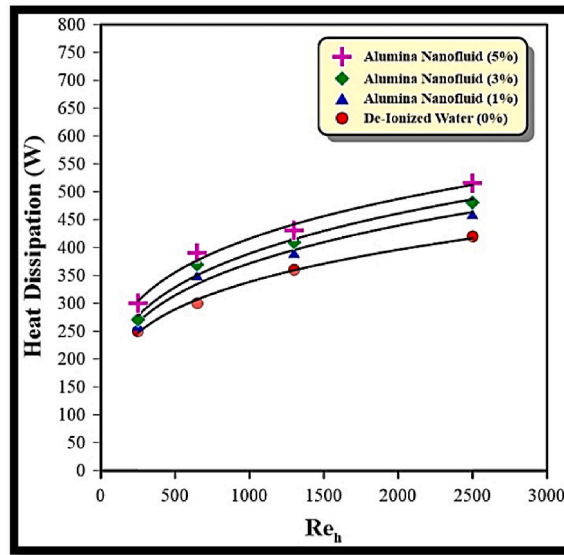


Fig. 9. The influence of (Re) on the heat dissipation of alumina-nanofluid at different concentrations of volume.

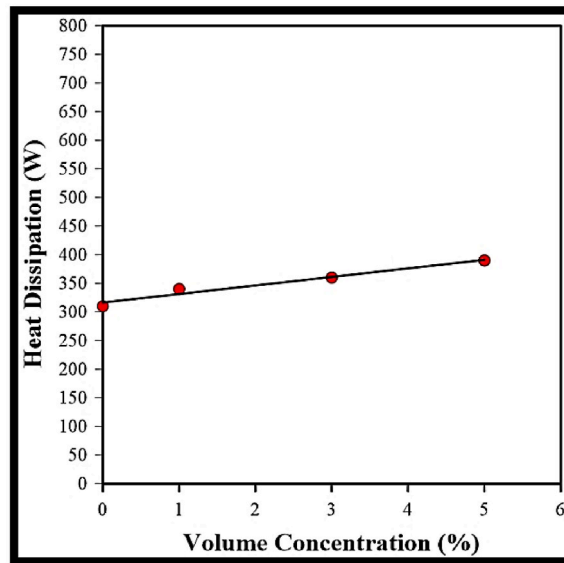


Fig. 10. Variation in heat dissipation as a function of alumina-nanofluid concentration.

$$\rho \left( u \frac{\partial v}{\partial x} + v \frac{\partial v}{\partial y} + w \frac{\partial v}{\partial z} \right) = - \frac{dp}{dy} + \mu \left( \frac{\partial^2 v}{\partial x^2} + \frac{\partial^2 v}{\partial y^2} + \frac{\partial^2 v}{\partial z^2} \right) \tag{3-3}$$

$$\rho \left( u \frac{\partial w}{\partial x} + v \frac{\partial w}{\partial y} + w \frac{\partial w}{\partial z} \right) = - \frac{dp}{dz} + \mu \left( \frac{\partial^2 w}{\partial x^2} + \frac{\partial^2 w}{\partial y^2} + \frac{\partial^2 w}{\partial z^2} \right) \tag{3-4}$$

3. Energy Equation

$$\rho C_p u \left( \frac{\partial u}{\partial x} + v \frac{\partial u}{\partial y} + w \frac{\partial u}{\partial z} \right) = k \left( \frac{\partial^2 T}{\partial x^2} + \frac{\partial^2 T}{\partial y^2} + \frac{\partial^2 T}{\partial z^2} \right) \tag{3-5}$$

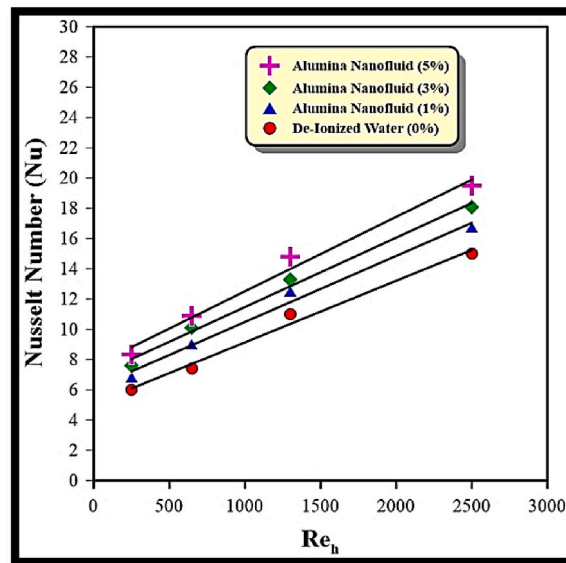


Fig. 11. Effect of inner Reynolds number on inner Nusselt number for alumina nanofluid at varied volume concentrations.

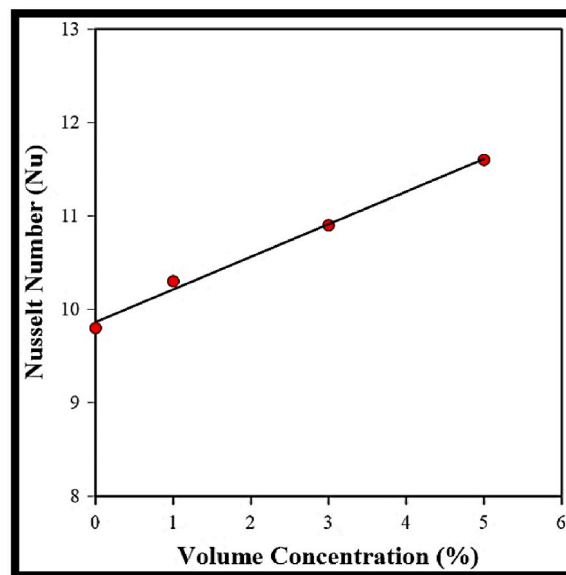


Fig. 12. Variation of the inner ( $Nu$ ) with alumina-nanofluid concentrations.

### 3.2. Turbulent flow

For turbulent flow in the annuli, the governing equations (continuity, momentum, energy, and transport equations). Equations representing different forms of laminar flow must be solved to find results [20].

## 4. Results and discussion

This part contains a detailed discussion of numerical findings. The heat transfer of inner tubes with and without fins is investigated. It is investigated how the addition of  $Al_2O_3$  nanoparticles to deionized water affects heat transmission. Numerical results represent three dimensional simulation of present heat exchanger with and without fins by using “K –  $\epsilon$  (RNG) model”. The inner and annuli sides feature laminar and turbulent flow, respectively. Several factors, such as nanoparticle volume concentration, Reynolds number, and axial distance ratio, are investigated numerically to determine the performance of the current heat exchanger.



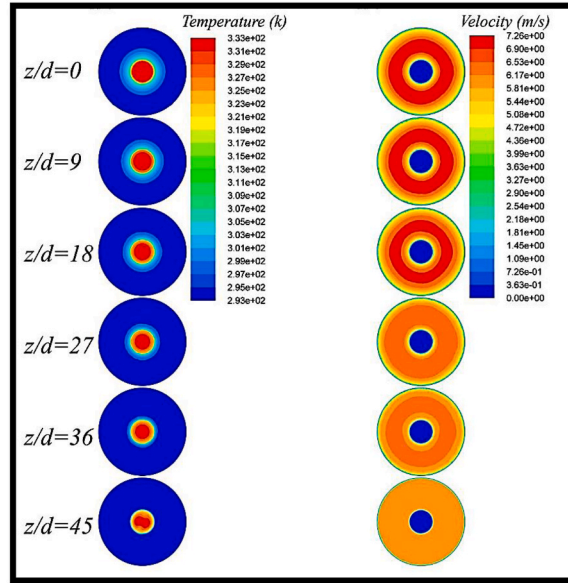


Fig. 13. “Temperature and velocity contours” at  $Re_h = 1400$ ,  $\dot{m}_c = 0.045\text{kg/sec}$ , and various axial distances for smooth tube heat exchanger.

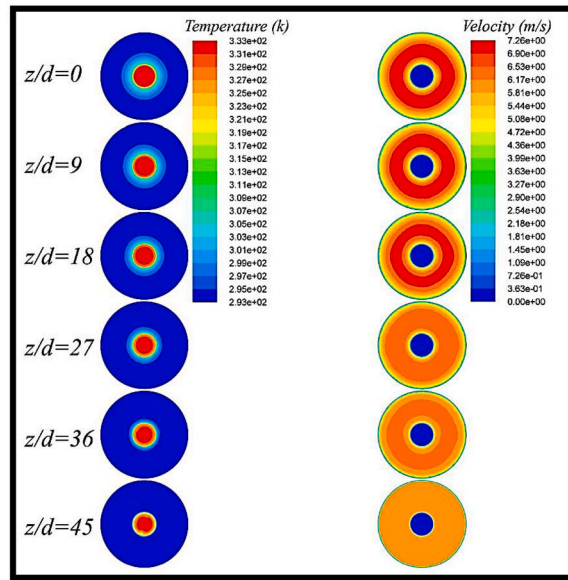


Fig. 14. “Temperature and velocity contours” at  $Re_h = 2000$ ,  $\dot{m}_c = 0.045\text{ kg/sec}$ , and various axial distances for smooth tube heat exchanger.

4.1. Validation of numerical results

A comparison has been done between the present work and the **Shah** equation result [23]. Fig. 3 shows the variation of the Nusselt number along the inner tube. It can be noted that the behavior of the present work (numerical data) regarding the hot side is the same as the **Shah** equation behavior. Plain tube data serves as a qualification for the facility and the procedure used over the range of Reynolds number studied. Fig. 4 shows a comparison of the Nusselt number ( $Nu$ ) of the experimental data with references results of **Sami et al.** [24]. The results shown in the figure reveals that the data for plain tube are in good agreement with the previous references results.

4.2. Heat exchanger performance without nanofluid

In the following paragraphs, the performance of heat exchangers is addressed in this section.

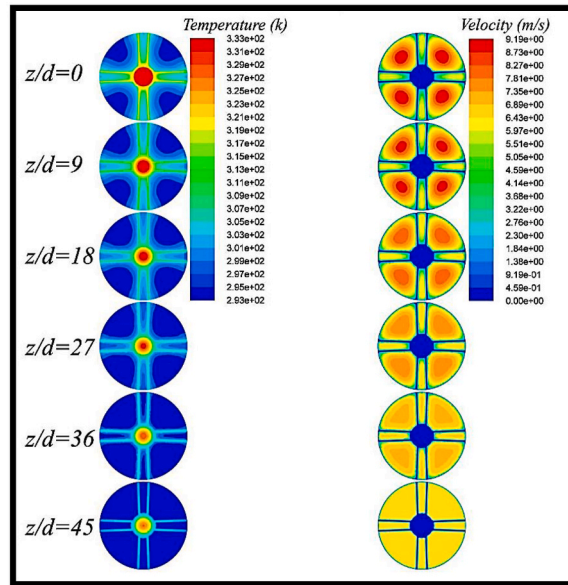


Fig. 15. “Temperature and velocity contours” at  $Re_h = 650$ ,  $\dot{m}_c = 0.045$  kg/sec, and various axial distances for finned tube heat exchanger.

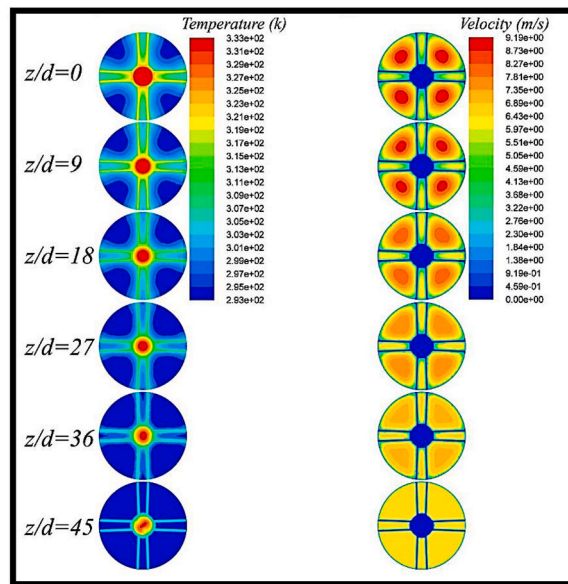


Fig. 16. “Temperature and velocity contours” at  $Re_h = 1300$ ,  $\dot{m}_c = 0.045$  kg/sec, and various axial distances for finned tube heat exchanger.

4.2.1. Influence of inner Reynolds number on heat dissipation

Figs. 5 and 6 depict the relationship between the Reynolds number of hot water as well as heat dissipation for finned and smooth tubes, respectively. It was carried out for a variety of cold water mass flow rates. Due to an increase in surface area, the finned tube’s heat dissipation is greater than that of flat tubes, as seen by these figures. The increase in heat dissipation is (2.3–3.1) times greater for the finned tube than for the smooth tube. According to these numbers, heat dissipation rises as the bulk flow rate of cold water increases.

4.2.2. Effect of inner Reynolds number on inner heat transfer coefficient

Figs. 7 and 8 illustrate the influence of varying Reynolds numbers for hot water on the inner heat transfer coefficient at varying Reynolds numbers for cold water. It can be shown that the heat transfer coefficient on the hot water side rises as a result of the turbulence caused by a rising water Reynolds number, suggesting a maximum increase of 67.3%. By raising the cold water’s Reynolds number, the hot water side heat transfer coefficient is reduced by four percent.

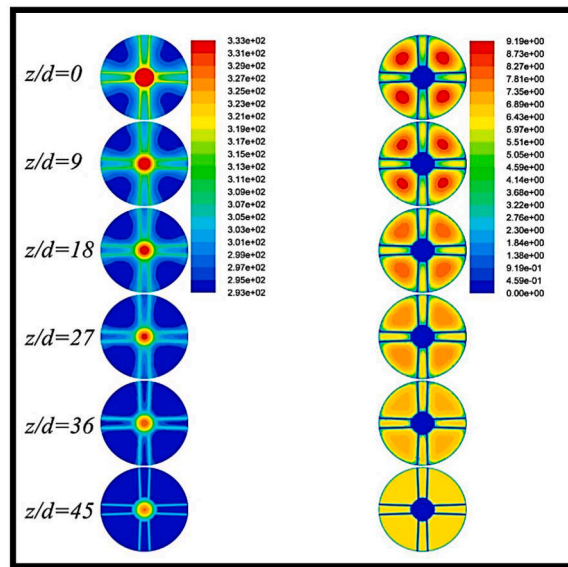


Fig. 17. “Temperature and velocity contours” at  $Re_h = 650$ ,  $\dot{m}_c = 0.045$  kg/sec, as well as a number of different axial distances for the finned tube heat exchanger using the alumina-nanofluid.

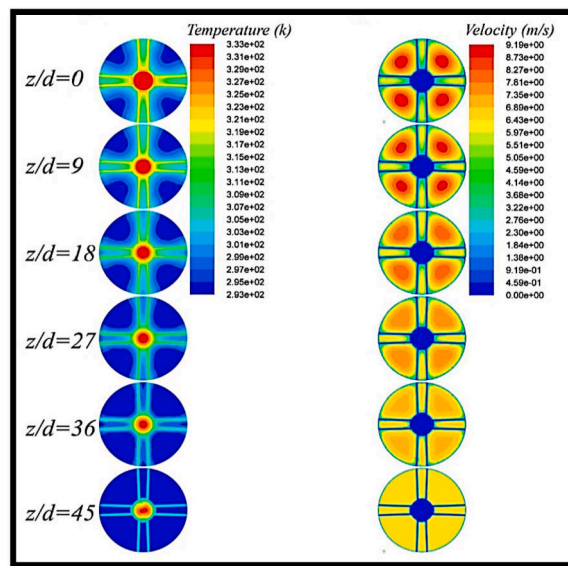


Fig. 18. Temperature and velocity contours at  $Re_h = 1300$ ,  $\dot{m}_c = 0.045$  kg/sec, as well as a number of different axial distances for the finned tube heat exchanger using the alumina-nanofluid.

### 4.3. Heat exchanger performance with nanofluid

The influence of volume concentration of nanoparticles on the performance of finned tube heat exchangers using nanofluids has been investigated. During the modeling of nanofluids, the Reynolds number of cold water was set to 13,000. In the next paragraphs, the thermal performance of heat exchangers containing nanofluids is explained.

#### 4.3.1. Effect of inner Reynolds number on heat dissipation

Fig. 9 depicts the relationship between alumina-nanofluid heat dissipation and the Reynolds number. With increasing nanofluid volume concentration and Reynolds number, it's clear that heat dissipation improves. Heat dissipation in alumina nanofluids is shown in Fig. 10 as a function of volume concentration.

#### 4.3.2. Influence of nanofluid on inner nusselt number

Using alumina-nanofluids, Fig. 11 shows how the Nusselt number changes with the Reynolds number. Figures like these show that

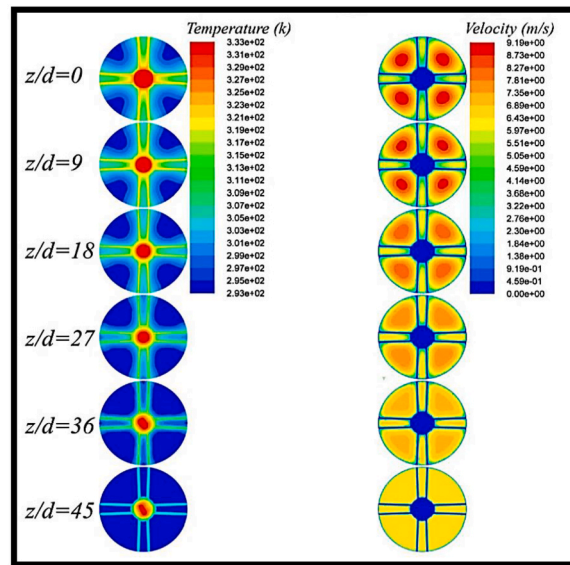


Fig. 19. Temperature and velocity contours at  $Re_h = 2000$ ,  $\dot{m}_c = 0.045$  kg/sec, as well as a number of different axial distances for the finned tube heat exchanger using the alumina-nanofluid.

the Nusselt number rises in direct proportion to both the Reynolds number and the nanoparticle volume concentration. The increased thermal conductivity and heat transfer coefficient of nanofluids are primarily responsible for this improvement. Volume concentration has an impact on the  $Nu$  in  $Al_2O_3$ -nanofluids, as seen in Fig. 12.

#### 4.4. Numerical contours analysis

The results of numerical simulation by ANSYS Fluent 20 are presented to show both the flow field and heat transfer of the present models. These findings are described in the sections that follow.

##### 4.4.1. Temperature and velocity contours

Figs. 13 and 14 depict the temperature and velocity contours of a smooth tube heat exchanger at varying water Reynolds numbers and axial distances. The greatest cold and hot water temperatures are seen at  $Z/d = 0$ , whereas the lowest temperatures are observed at  $Z/d = 45$ . Observing  $Z/d = 18$  demonstrates that a change in the water's Reynolds number will not have a substantial influence on the cold water side. The cold water in the annuli seems to be the primary cause of this phenomenon. The velocity contours in these figures demonstrate that the velocity distribution at the cold water entrance at  $Z/d = 45$  is uniform. It will also tend to decrease within the heat exchanger at the inner and outer tube walls, as shown by the  $Z/d$  value decreasing from 36 to 0.

Figs. 15 and 16 illustrate the temperature and velocity profiles of a finned tube heat exchanger for specified hot water Reynolds numbers and cold water mass flow rates at different axial distance ratios. Results demonstrated a considerable increase in heat transmission for  $Z/d$  values between 0 and 45 for both the cold water and hot water sides. On both sides, the impact of fins on heat transfer is evident. The behavior of heat transfer enhancement for " $Z/d = 27$ " and " $\dot{m}_c = 0.025$  kg/s" is evident as the water Reynolds number increases. As demonstrated for " $Z/d = 18$ " for both situations, an increase " $\dot{m}_c$  to 0.045 kg/s" tends to raise the hot water side temperature difference along the axial distance while lowering the cold water side temperature difference. These velocity contours demonstrate that the velocity of cold water is uniform at " $Z/d = 45$ ". However, it increases from 36 to 0 in the center between every two pairs of fins at  $Z/d$ . In these figures, the influence of the wall on lowering the velocity on the cold water and hot water sides is evident.

The temperature and velocity contours of a finned tube heat exchanger using nanofluids are shown in Figs. 17–18, respectively. It is important to take notice that the improvement of heat transfer on the cold water side is seen for  $Z/d$  values ranging from 0 to 18. But in terms of the hot water side of things,  $Z/d$  ranges from 27 to 45. In spite of the fact that the increase in thermal conductivity is rather modest, the primary cause of this boost is found in the thermophysical characteristics of nanofluids. This enhancement in heat transfer behavior is able to be improved to a greater extent by an increase in the thermal conductivity of the base fluid (see Fig. 19).

## 5. Conclusions

In this work, a numerical investigation of the heat transfer in a finned, double-pipe heat exchanger implanted on the inner tube's outside surface was provided. The study is carried out with a new technique that includes nanofluid to enhance heat transfer. The main conclusion of this research may be summed up as follows:

1. The improvement in heat transmission is seen when fins are added to the inner tube's outside surface in the current heat exchanger. This improvement is seen in the values of the cold water heat transfer coefficient and heat dissipation, which are (2.3–3.1) and correspondingly (1.6–2) times that of a smooth tube. The temperature differential on the hot water side is immediately connected

to the mass flow rate of cold water and decreases by (66%) as the hot water Reynolds number increases.

2. The temperature differential on the cold water side is exactly related to the hot water Reynolds number and decreases by 57% as the cold water mass flow rate increases.
3. By adding nanoparticles to the base fluid, the heat exchanger's current heat transfer coefficient is markedly increased. At a volume concentration of 5%, the greatest boost reported for alumina nanoparticles is twenty percent.
4. Adopting fins on the outside surface of the inner tube significantly improved the efficacy of heat exchangers.
5. The addition of fins improved heat dissipation via the heat exchanger, according to the results of the numerical simulation. An increase in cold water mass flow rates and hot water Reynolds numbers has been seen in this model.
6. The current heat exchanger may be accurately predicted using the FLUENT program, which simulates both heat transfer and fluid movement.

#### Author statement

I have participated sufficiently in the conception and design of this work or the analysis and interpretation of the data, as well as the writing of the manuscript, to take public responsibility for it. I believe the manuscript represents valid work. I have reviewed the final version, and I approve it for publication. Neither this manuscript nor one with substantially similar content under my authorship has been published or is being considered for publication elsewhere, except as may be described in an attachment to this statement.

#### Declaration of competing interest

The authors declare that they have no known competing financial interests or personal relationships that could have appeared to influence the work reported in this paper.

#### Data availability

Data will be made available on request.

#### References

- [1] Ramesh K. Shah, Dušan P. Sekulic, *Fundamentals of Heat Exchanger Design*, John Wiley & Sons, New York, 2003.
- [2] A. Dewan, P. Mahanta<sup>1</sup>, K. Sumithra Raju, P. Suresh Kumar, Review of passive heat transfer augmentation techniques, in: *Proceedings of the Institution of Mechanical Engineers*, 218, 2004, pp. 509–527. Part A: Journal of Power and Energy.
- [3] K. Sivakumar, K. Rajan, Performance analysis of heat transfer and effectiveness on laminar flow with effect of various flow rates, *Int. J. ChemTech Res.* 7 (No.6) (2014–2015) 2580–2587.
- [4] N. Sahiti, F. Durst, A. Dewan, Heat transfer enhancement by pin elements, *Int. J. Heat Mass Tran.* 48 (2005) 4738–4747.
- [5] Shuai Shi, Yan Chang-qi, "Numerical Study of Heat Transfer and Pressure Drop of Integral Pin-Fin Tubes", 978–1, 2011, pp. 4244–6255, 1/11.
- [6] Dong H. Lee, Jin M. Jung, Jong H. Ha, Young I. Cho, Improvement of heat transfer with perforated circular holes in finned tubes of air cooled heat exchanger, *Int. Commun. Heat Mass Tran.* 39 (2012) 161–166.
- [7] N. Nagarani, K. Mayilsamy, Experimental heat transfer analysis on annular circular and elliptical fins, *Int. J. Eng. Sci. Technol.* 2 (7) (2010) 2839–2845.
- [8] S. Senthilraja, K.C.K. Vijayakumar, Analysis of heat transfer coefficient of CuO/water nanofluid using double pipe heat exchanger, *Int. J. Eng. Res. Technol.* 6 (No. 5) (2013) 675–680.
- [9] S. Zeinali Heris, M. Nasr Esfahany, S. Gh Etamad, Heat transfer enhancement of nanofluid laminar flow, in: *18<sup>th</sup> Annual (International) Mechanical Engineering Conference*, 2006.
- [10] W.Y. Lai, B. Duculescu, Phelan, "Proceedings of ASME International Mechanical Engineering Congress and Exposition", 2006. Chicago, USA.
- [11] B. Farajollahi, S. Gh Etamad, M. Hojjat, Heat transfer of nanofluids in A shell and tube heat exchanger, *Int. J. Heat Mass Tran.* 53 (2010) 12–17.
- [12] E. Esmaeilzadeh, H. Almohammadi, Sh Nasiri Vatan, A.N. Omran, Experimental investigation of hydrodynamics and heat transfer characteristics of -/water under laminar flow inside a horizontal tube, *Int. J. Therm. Sci.* 63 (2013) 31–37.
- [13] V. Mathanraj, Velaga Leela Krishna, Jampana Lakshmi Venkanna Babu, S. Arul Kumar, Experimental investigation on heat transfer in double pipe heat exchanger employing triangular fins, *IOP Conf. Ser. Mater. Sci. Eng.* 402 (2018), 012137.
- [14] J.I. Córcoles, J.D. Moya-Rico, A.E. Molina, J.A. Almendros-Ibáñez, Numerical and experimental study of the heat transfer process in a double pipe heat exchanger with inner corrugated tubes, *Int. J. Therm. Sci.* 158 (December 2020), 106526.
- [15] Mahmud H. Ali, Rawand E. Jalal, Experimental Investigation of Heat Transfer Enhancement in a Double Pipe Heat Exchanger with a Twisted Inner Pipe", *Heat Transfer*, December 2021, pp. 8121–8133. Volume50, Issue8.
- [16] Mojtaba Fadaei, Mohsen Izadi, Ehsanolah Assareh, Ershadi Ali, Conjugated non-Newtonian phase change process in a shell and tube heat exchanger: a parametric-geometric analysis, *Appl. Therm. Eng.* 220 (5 February 2023), 119795, <https://doi.org/10.1016/j.applthermaleng.2022.119795>.
- [17] Do Huu-Quan, Ali Mohammad Rostami, Mozafar Shokri Rad, Mohsen Izadi, Hajjar Ahmad, Qingang Xiong, 3D numerical investigation of turbulent forced convection in a double-pipe heat exchanger with flat inner pipe, *Appl. Therm. Eng.* 182 (2021), 116106, <https://doi.org/10.1016/j.applthermaleng.2020.116106>.
- [18] P. Kumar, A CFD study of heat transfer enhancement in pipe flow with Al<sub>2</sub>O<sub>3</sub> nanofluid, *World Academy of Science, Engineering and Technology* 57 (2011) 746–750.
- [19] H.K. Versteeg, W. Malalasekera, *An Introduction to Computational Fluid Dynamics-The Finite Volume Method*, Longman group Ltd., 1995.
- [20] ANSYS Fluent User's Guide, ANSYS Inc., South Pointe 275 Technology Drive Canonsburg, 2011.
- [21] Lars Davidson, *An Introduction to Turbulence Models*, Department of Thermo and Fluid Dynamics, Chalmers University of Technology, Sweden, 2015.
- [22] M. Izadi, M.M. Shahmardan, M.J. Maghrebi, A. Behzadmehr, NUMERICAL STUDY OF DEVELOPED LAMINAR MIXED CONVECTION OF Al<sub>2</sub>O<sub>3</sub>/WATER NANOFLUID IN AN ANNULUS, *Chem. Eng. Commun.* 200 (7) (2013) 878–894, <https://doi.org/10.1080/00986445.2012.723077>.
- [23] R.K. Shah, *Thermal Entry Length Solutions for the Circular Tubes and Parallel Plates* Indian Institute Of Technology, Bombay, 1975, pp. 11–75.
- [24] P. Murugesan, K. Mayilsamy, S. Suresh, P.S.S. Srinivasan, Heat transfer and pressure drop characteristics in a circular tube fitted with and without V-cut twisted tape insert, *Int. Commun. Heat Mass Tran.* 38 (3) (2011) 329–334.